arXiv:cond-mat/0211294v1 [cond-mat.soft] 14 Nov 2002

Macroscopic dynamics of a Bose-Einstein condensate containing a vortex lattice

Marco Cozzini and Sandro Stringari
Dipartimento di Fisica, Università di Trento and BEC-INFM, I-38050 Povo, Italy

(Dated: February 1, 2008)

Starting from the equations of rotational hydrodynamics we study the macroscopic behaviour of a trapped Bose-Einstein condensate containing a large number of vortices. The stationary configurations of the system, the frequencies of the collective excitations and the expansion of the condensate are investigated as a function of the angular velocity of the vortex lattice. The time evolution of the condensate and of the lattice geometry induced by a sudden deformation of the trap is also discussed and compared with the recent experimental results of P. Engels *et al.*, Phys. Rev. Lett. **89**, 100403 (2002).

PACS numbers: 03.75.Fi, 32.80.Lg

After their experimental realization [1, 2] quantized vortices have become a popular subjet of research in the field of ultra cold gases (see for example [3]). More recently, special emphasis has been given to the study of configurations containing a large number of vortical lines (vortex lattices) [4, 5]. An important motivation is due to the possibility of reaching critical regimes of high angular velocities where the degeneracy of the single particle levels gives rise to new quantum configurations, analog to the quantum Hall effect [6, 7, 8, 9].

The purpose of the present work is to describe the macroscopic behaviour of a Bose-Einstein condensate containing a vortex lattice in the so called Thomas-Fermi regime [10], where the interaction energy is much larger than the trapping oscillator energies. A complementary investigation concerns the dynamic behaviour of vortex lines, where interactions play a role at a more microscopic scale [11, 12].

In the presence of a large number of vortex lines a useful concept is the so called diffused vorticity given by

$$\boldsymbol{\nabla}\wedge\mathbf{v} = 2\,\boldsymbol{\Omega}\ , \tag{1}$$

where $\mathbf{v}$ is the velocity field of the fluid and $\boldsymbol{\Omega}$ is assumed to be uniform. In terms of the density n_v of the vortex lines per unit surface one has $n_v = 2\,\Omega\,M/h$, where M is the atomic mass. The quantity $\boldsymbol{\Omega}$ corresponds to the angular velocity of the sample. The concept of diffused vorticity is adequate to describe the dynamics at macroscopic distances, larger than the average distance $n_v^{-1/2}$ between vortices.

The macroscopic description is provided by the equations of rotational hydrodynamics

$$\frac{\partial n}{\partial t} + \boldsymbol{\nabla}\cdot(n\mathbf{v}) = 0\ , \tag{2}$$

$$M\frac{\partial\mathbf{v}}{\partial t} + \boldsymbol{\nabla}\left(\frac{Mv^2}{2} + V_{\rm ext} + gn\right) = M\mathbf{v}\wedge(\boldsymbol{\nabla}\wedge\mathbf{v}) \tag{3}$$

written in the laboratory frame, where $n(\mathbf{r},t)$ is the spatial density, $\mathbf{v}(\mathbf{r},t)$ is the velocity field, $V_{\rm ext}$ is the external potential and $g = 4\pi\hbar^2 a/M$ is the coupling costant expressed in terms of the s-wave scattering length a. These equations generalize the usual equations of irrotational hydrodynamics ($\boldsymbol{\nabla}\wedge\mathbf{v} = 0$), which have been successfully applied to study the collective oscillations of the condensates in the absence of vortex lines [14]. It is worth noticing that the hydrodynamic theory is well suited to study also non linear effects, including the expansion of the gas after release of the confining trap.

For an axi-symmetric harmonic potential $V_{\rm ext} = M\,[\omega_\perp^2\,(x^2+y^2) + \omega_z^2\,z^2]/2$ the equilibrium solutions of Eqs. (2) and (3) have the form $\mathbf{v}_0 = \boldsymbol{\Omega_0}\wedge\mathbf{r}$ and

$$n_0(\mathbf{r}) = \frac{1}{g}\left\{\mu - \frac{M}{2}\left[\tilde\omega_\perp^2\,(x^2+y^2) + \omega_z^2\,z^2\right]\right\}\ , \tag{4}$$

where the effective frequency given by $\tilde\omega_\perp^2 = \omega_\perp^2 - \Omega_0^2$ originates from the centrifugal effect and

$$\mu = \mu_0\,\left[1 - \left(\frac{\Omega_0}{\omega_\perp}\right)^2\right]^{2/5} \tag{5}$$

is the chemical potential. In the previous equation $\mu_0 = (\hbar\omega_{\rm ho}/2)\,(15Na/a_{\rm ho})^{2/5}$ is the chemical potential in the absence of rotation, $\omega_{\rm ho} = (\omega_\perp^2\omega_z)^{1/3}$ is the average oscillator frequency, $a_{\rm ho} = \sqrt{\hbar/M\omega_{\rm ho}}$ is the corresponding oscillator length and N is number of atoms. These stationary solutions are defined only for $\Omega_0 < \omega_\perp$. The density profile (4) exhibits a typical bulge effect produced by the centrifugal force, giving rise to the angular velocity dependence

$$\frac{R_\perp}{R_z} = \frac{\omega_z}{\sqrt{\omega_\perp^2 - \Omega_0^2}} \tag{6}$$

for the aspect ratio, where $R_\perp$ and R_z are, respectively, the Thomas-Fermi radii of the atomic cloud in the radial and axial directions. Result (6) can be used to deduce the value of Ω_0 from the *in situ* measurement of the aspect ratio. In Ref. [5] values up to $\Omega_0/\omega_\perp = 0.95$ have been obtained. In that experiment the condensate takes a pancake form even if the confining trap has a cigar shape ($\omega_z < \omega_\perp$).

The angular momentum per particle carried by the system is given by

$$\langle l_z \rangle = M\Omega_0 \langle x^2 + y^2 \rangle = \frac{4}{7}\,\frac{\Omega_0}{\omega_\perp^2 - \Omega_0^2}\,\mu \qquad (7)$$

and becomes larger and larger as $\Omega_0 \to \omega_\perp$.

The collective oscillations of the condensate are obtained by looking for the linearized solutions of Eqs. (2) and (3) in the form $n = n_0 + \delta n$ and $\mathbf{v} = \mathbf{v}_0 + \delta\mathbf{v}$ with δn and $\delta\mathbf{v} \sim e^{-i\omega t}$.

If one chooses $\delta n = a_\pm (x \pm iy)^2$, $\delta\mathbf{v} = \alpha_\pm \boldsymbol{\nabla}(x \pm iy)^2$, corresponding to quadrupole excitations with $m = \pm 2$ where m is the third component of angular momentum, one easily finds the dispersion law [21]

$$\omega(m = \pm 2) = \sqrt{2\,\omega_\perp^2 - \Omega_0^2} \pm \Omega_0 \ . \qquad (8)$$

These frequencies have been directly measured in the experiment of [5], confirming with high accuracy the predictions of theory. The splitting $2\,\Omega_0$ between the two frequencies agrees with the sum rule result [16]

$$\omega(m = +2) - \omega(m = -2) = \frac{2}{M}\,\frac{\langle l_z \rangle}{\langle x^2 + y^2 \rangle} \ , \qquad (9)$$

as can be seen using the rigid body expression (7) for the angular momentum.

When $\Omega_0 \to \omega_\perp$ one finds $\omega(m = +2) \to 2\omega_\perp$, while $\omega(m = -2) \to 0$, reflecting the tendency of the system to become unstable against static quadrupole deformations.

In addition to the $m = \pm 2$ oscillations, it is interesting to discuss the behaviour of the $m = 0$ modes [22]. These result from the coupling between the axial and radial motion of the condensate. By looking for solutions of the form $\delta n(\mathbf{r}) = a_0 + a_\perp(x^2 + y^2) + a_z\,z^2$ and $\delta\mathbf{v}(\mathbf{r}) = \delta\boldsymbol{\Omega} \wedge \mathbf{r} + \boldsymbol{\nabla}[\alpha_\perp(x^2 + y^2) + \alpha_z\,z^2]$ one finds that the two decoupled frequencies are given by

$$\begin{aligned}\omega^2(m = 0) \ &= \qquad (10)\\ &2\,\omega_\perp^2 + \tfrac{3}{2}\,\omega_z^2 \pm \tfrac{1}{2}\sqrt{16\,\omega_\perp^4 + 9\,\omega_z^4 - 16\,\omega_z^2\,\omega_\perp^2 - 8\,\omega_z^2\,\Omega_0^2}\ .\end{aligned}$$

When $\Omega_0 = 0$ one recovers the solutions of [14], while for $\Omega_0 \to \omega_\perp$ the two frequencies approach the value $2\,\omega_\perp$ (radial compressional mode) and $\sqrt{3}\,\omega_z$ (axial compressional mode). The latter value coincides with the frequency predicted by theory for a pancake geometry ($\omega_z \gg \omega_\perp$) in the absence of vortices.

The tendency of the system to become unstable against a quadrupole deformation when $\Omega_0 \to \omega_\perp$ has been used in the recent experiment of [15] to induce large deformations in the condensate and to explore the consequences on the geometry of the vortex lattice.

In the presence of a static deformation of the trap

$$\delta V_{\rm ext} = \frac{M}{2}\,\omega_\perp^2 \epsilon (x^2 - y^2) \qquad (11)$$

the stationary solutions of the hydrodynamic equations (2) and (3) in the laboratory frame change in a quite interesting way. On the one hand the velocity field takes the form

$$\mathbf{v}_0(\mathbf{r}) = \boldsymbol{\Omega_0} \wedge \mathbf{r} + \alpha \boldsymbol{\nabla}(xy) \ , \qquad (12)$$

containing a crucial irrotational component fixed by the parameter α. On the other hand the equilibrium profile assumes the deformed shape

$$n_0(\mathbf{r}) = \frac{1}{g}\left[\mu - \frac{M}{2}\left(\tilde{\omega}_x^2\,x^2 + \tilde{\omega}_y^2\,y^2 + \omega_z^2\,z^2\right)\right] \ , \qquad (13)$$

with the effective frequencies defined by $\tilde{\omega}_{x,y}^2 = \omega_{x,y}^2 + \alpha^2 - \Omega_0^2$ and the chemical potential given by $\mu = \mu_0(\tilde{\omega}_x\tilde{\omega}_y/\omega_x\omega_y)^{2/5}$. Use of the equation of continuity yields the following third order equation for α

$$\alpha^3 + \alpha(\omega_\perp^2 - \Omega_0^2) - \epsilon\omega_\perp^2\Omega_0 = 0 \ , \qquad (14)$$

whose solution, expressed in terms of the deformation of the condensate

$$\delta = \frac{\langle y^2 - x^2 \rangle}{\langle x^2 + y^2 \rangle} = \frac{\alpha}{\Omega_0} \ , \qquad (15)$$

is reported in Fig. 1 for the value $\epsilon = 0.036$. The other solutions of the third order equation (14) should be excluded because they correspond to negative values of $\tilde{\omega}_{x,y}^2$. This differs from the situation of Ref. [18], where only irrotational flow was considered and more stationary solutions were found to be available in the rotating frame. For $\epsilon \neq 0$, Fig. 1 shows that, differently from the axisymmetric case, a deformed system can support values of Ω_0 larger than $\omega_\perp$, the irrotational term of Eq. (12) providing the crucial compensation to the centrifugal effect

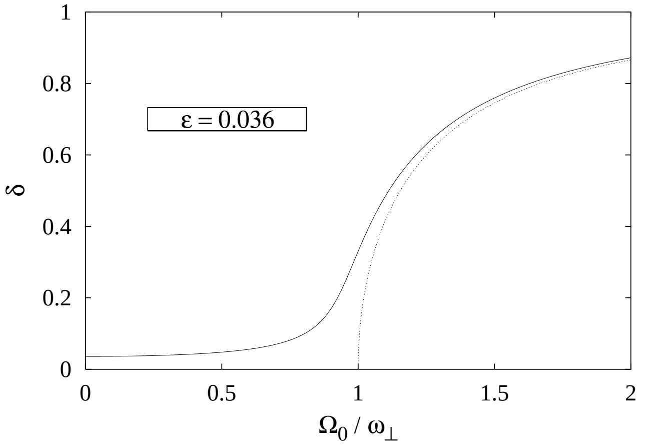

FIG. 1: Deformation $\delta = \alpha/\Omega_0$ of the cloud for the steady-state solutions of Eqs. (2) and (3) as a function of the angular velocity Ω_0 of the vortex lattice, for a fixed value $\epsilon = 0.036$ of the trap deformation. The dotted line is the asymptotic solution for $\epsilon \to 0$.

generated by the rotational component. When $\epsilon \to 0$ and $\Omega_0 \geq \omega_\perp$ one finds $\tilde{\omega}_{x,y}^2 \to 0$ and the branch approaches the asymptotic solution $\delta = \sqrt{1 - (\omega_\perp/\Omega_0)^2}$.

In the experiment of [15] the static deformation (11) was switched on suddenly at some initial time $t = 0$. This produces a time tependent perturbation which drives the system far from the initial axi-symmetric configuration. In the following we will discuss the prediction of Eqs. (2) and (3) for the time evolution of the condensate shape as well as of the vortex lines which are assumed to follow the motion of the fluid. The equations are easily solved in the non linear regime by looking for the ansatz

$$n = a_0 + a_x x^2 + a_y y^2 + a_z z^2 + a_{xy} xy \qquad (16)$$
$$\mathbf{v} = \mathbf{\Omega} \wedge \mathbf{r} + \boldsymbol{\nabla}(\alpha_x x^2 + \alpha_y y^2 + \alpha_z z^2 + \alpha_{xy} xy), \qquad (17)$$

where now Ω, as well as the coefficients a_i and α_i, is time dependent. In Fig. 2(a) we report the predictions for the angle between the principal axis of the condensate and the y axis of the trap, with the initial value of the angular velocity $\Omega_0 = 0.95\,\omega_\perp$. The angle first increases fast following the direction of the vortex flow. This happens because for short times the perturbation excites with equal strength both the $m = +2$ and $m = -2$ modes and hence the system exhibits a precession with angular velocity proportional to $\omega(m = +2) - \omega(m = -2)$. For longer times the response is governed by the static effect and is dominated by the $m = -2$ mode, producing a precession in the opposite direction whose period becomes longer and longer as the value of ϵ decreases. The deformation of the condensate as a function of time is plotted in Fig. 2(b) for the same conditions: rather large values are reached, in agreement with the experimental findings of [15]. For example at $t \simeq 2.5\,T_\perp$ the authors of [15] report the value $\delta \simeq 0.4$. The coupling with the fast $m = +2$ mode is evident in both figures and results in the small oscillations of higher frequency.

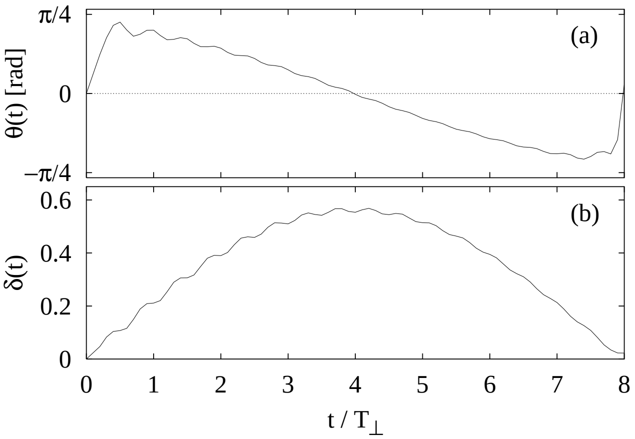

FIG. 2: Time dependence of the condensate after switching on the trap deformation with $\epsilon = 0.036$: (a) evolution of the angle $\theta(t)$ between the principal axis of the cloud and of the trap in the $x - y$ plane; (b) evolution of the cloud deformation $\delta(t)$. The axial frequency of the trap is $\omega_z = 0.65\,\omega_\perp$, while the initial configuration is the stationary solution for $\epsilon = 0$ and $\Omega = 0.95\,\omega_\perp$. Time is measured in units of $T_\perp = 2\pi/\omega_\perp$.

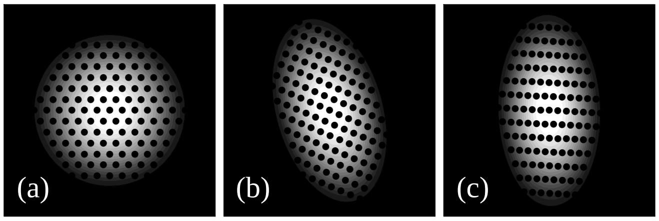

FIG. 3: Evolution of the vortex lattice after switching on the trap deformation $\epsilon = 0.036$: (a) $t = 0$, (b) $t = 2.8\,T_\perp$, (c) $t = 3.9\,T_\perp$. The peculiar geometry shown in (c) appears when the cloud deformation δ is large and one of the lattice vector is aligned along the short axis of the condensate. The trap parameters are the same as in Fig. 2.

Once the solutions of the hydrodynamic equations are known one can also study the time evolution of the vortex lines wich are assumed to move following the velocity field $\mathbf{v}$ (Fig. 3). We have initially assumed [Fig. 3(a)] an hexagonal geometry (Abrikosov lattice [19]). In the absence of deformation the vortex lines rotate rigidly with angular velocity Ω_0. However, once the deformation of the condensate takes place, the vortex lattice changes its geometry since it is forced to follow the stream lines of the velocity flow (17) wich contains an irrotational component. For example, in Fig. 3(b) one sees the formation of a near orthorhombic lattice, while for large deformations one observes peculiar structures characterized by the compression of vortex lines along the short radius [Fig. 3(c)]. In our description the vortex lines are just points of the fluid moving with velocity $\mathbf{v}$, so we do not account for the possible deformation of the density profiles induced by the vicinity of the vortex lines. These effects are expected to give rise to a significant suppression of the density in the region between two vortices when their relative distance becomes small, with the appearence of stripe like configurations as observed in the experiments of [15] and recently discussed in [13].

An important role in the experimental detection of vortices is played by the expansion of the condensate. The vortex cores are indeed too small to be imaged *in situ*. It is therefore important to look at the behaviour of the condensate after the sudden release of the trap. This can be investigated by solving the hydrodynamic equations (2) and (3) setting $V_{\rm ext} = 0$ at the release time. The general solution is still given by the form (16) and (17). We have first studied the time dependence of the aspect ratio (6), starting from an axisymmetric configuration ($\epsilon = 0$). Using the trapping parameters of Ref. [15] we find that $R_\perp/R_z$ increases in time (see Fig. 4). This dramatically differs from the expansion of a non rotating condensate, which would instead transform a pancake cloud into a cigar shape one. This behaviour is the

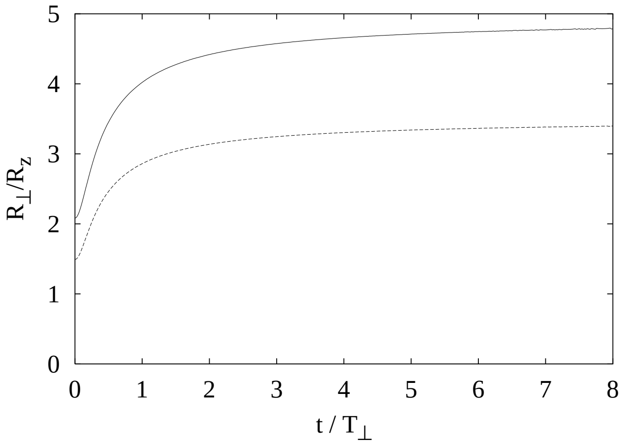

FIG. 4: Time evolution of the aspect ratio (6) after releasing the axisymmetric trap for a condensate rotating at $\Omega_0 = 0.95\,\omega_\perp$ (solid line) and $\Omega_0 = 0.90\,\omega_\perp$ (dashed line). The anisotropy of the trap is $\lambda = \omega_z/\omega_\perp = 0.65$.

consequence of the large radial rotational kinetic energy, which produces a fast expansion in the radial direction, and becomes more and more pronounced as $\Omega_0 \to \omega_\perp$. We have also investigated the time evolution of the cloud deformation $\delta(t)$ in the $x-y$ plane, by switching off the confining potential when the perturbation (11) has produced a sizable condensate deformation [see Fig. 2(b)]. Using the experimetal parameters of [15] we find that the value of the condensate deformation remains almost constant during the expansion. This is again the consequence of the centrifugal effect, which is stronger in the direction of the long axis and compensates the effects of the pressure gradient.

Let us finally discuss the conditions of applicability of the Thomas-Fermi approximation used in the present work. If Ω_0 becomes too close to $\omega_\perp$ the condition $\mu \gg \hbar\omega_\perp, \hbar\omega_z$ required to apply the Thomas-Fermi approximation is no longer valid [see Eq. (5)]. In particular if $\mu \simeq \hbar\omega_\perp$ the size of the vortex core, fixed by the healing length $\xi = \hbar/\sqrt{2M\mu}$, becomes comparable to the average distance between vortices, fixed by the so called effective magnetic length $\ell_{\Omega_0} = \sqrt{\hbar/2M\Omega_0}$. In fact one has $\xi/\ell_{\Omega_0} = \sqrt{\hbar\Omega_0/\mu} \simeq \sqrt{\hbar\omega_\perp/\mu}$. In the experimental conditions of Ref. [15] one has $\mu_0 \simeq 27\,\hbar\omega_{\rm ho}$ and the Thomas-Fermi approximation is well satisfied also for $\Omega_0 = 0.95\,\omega_\perp$. Deviations from the Thomas-Fermi regime require smaller values of μ_0 and/or larger values of $\Omega_0/\omega_\perp$ and should show up in a different behaviour of the collecitve frequencies.

Let us also mention that in order to observe quantum Hall features one should reach even more extreme conditions, where the filling factor $\nu = N/N_v$, given by the ratio between the number of atoms and the number of vortices, is of the order of unity [23]. Under these conditions the low frequency oscillations in the rotating frame are expected to exhibit a chiral behaviour [20], similar to what happens to the edge excitations in the quantum Hall effect.

In conclusion, we have studied the stationary configurations and the dynamics of a Bose-Einstein condensate both in an axisymmetric and in an anisotropic static trap, using the equations of rotational hydrodynamic and the concept of diffused vorticity. Special emphasis has been given to the collective oscillations, wich turn out to be significantly affected by the rotation of the cloud. In addition, our macroscopic description gives valuable insight on the evolution of the vortex lines recently observed in [15].

Useful discussions with F. Chevy, E. A. Cornell and P. Engels are acknowledged. This work was supported by the Ministero dell'Università e della Ricerca Scientifica e Tecnologica (MURST).

---

[1] B. P. Anderson *et al.*, Phys. Rev. Lett. **85**, 2857 (2000).
[2] K. W. Madison *et al.*, Phys. Rev. Lett. **84**, 806 (2000).
[3] A. L. Fetter and A. A. Svidzinsky, J. Phys.: Condens. Matter **13**, R135 (2001).
[4] M. R. Matthews *et al.*, Phys. Rev. Lett. **83**, 2498 (1999).
[5] P. C. Haljan *et al.*, Phys. Rev. Lett. **87**, 210403 (2001).
[6] N. K. Wilkin and J. M. F. Gunn, Phys. Rev. Lett. **84**, 6 (2000).
[7] B. Paredes *et al.*, Phys. Rev. Lett. **87**, 010402 (2001).
[8] Tin-Lun Ho, Phys. Rev. Lett. **87**, 060403 (2001).
[9] J. Sinova, C. B. Hanna and A. H. MacDonald, Phys. Rev. Lett. **89**, 030403 (2002).
[10] F. Dalfovo *et al.*, Rev. of Mod. Phys. **71**, 463 (1999).
[11] J. R. Anglin and M. Crescimanno, cond-mat/0210063.
[12] U. R. Fischer and G. Baym, cond-mat/0111443.
[13] E. J. Mueller, Tin-Lun Ho, cond-mat/0210276.
[14] S. Stringari, Phys. Rev. Lett. **77**, 2360 (1996).
[15] P. Engels *et al.*, Phys. Rev. Lett. **89**, 100403 (2002).
[16] F. Zambelli, S. Stringari, Phys. Rev. Lett. **81**, 1754 (1998).
[17] F. Chevy, S. Stringari, in preparation.
[18] A. Recati, F. Zambelli, S. Stringari, Phys. Rev. Lett. **86**, 377 (2001).
[19] A. A. Abrikosov, JETP **32**, 1442 (1957), Soviet Phys. JETP **5**, 1174 (1957).
[20] M. A. Cazalilla, cond-mat/0207715.
[21] Eq. (8) can be generalized to excitations of higher multipolarity ℓ and $m = \pm\ell$. One finds [17] $\omega_\pm = \sqrt{\ell\,\omega_\perp^2 - (\ell-1)\,\Omega_0^2} \pm (\ell-1)\,\Omega_0$.
[22] The $m = \pm 1$ modes, wich involve a dynamic coupling with the rotation of the axis of vorticity (tilting mode), will be discussed elsewhere [17].
[23] For example, assuming a 3-D Thomas-Fermi profile, one finds $\nu = (2/15)(\mu/\hbar\Omega_0)(R_z/a)$ and hence $\nu \gg 1$ even if $\mu \simeq \hbar\Omega_0$.